

RSC Advances



This is an *Accepted Manuscript*, which has been through the Royal Society of Chemistry peer review process and has been accepted for publication.

Accepted Manuscripts are published online shortly after acceptance, before technical editing, formatting and proof reading. Using this free service, authors can make their results available to the community, in citable form, before we publish the edited article. This *Accepted Manuscript* will be replaced by the edited, formatted and paginated article as soon as this is available.

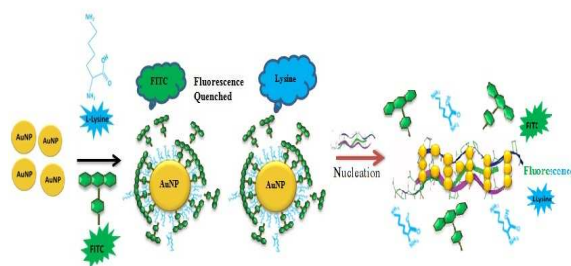
You can find more information about *Accepted Manuscripts* in the [Information for Authors](#).

Please note that technical editing may introduce minor changes to the text and/or graphics, which may alter content. The journal's standard [Terms & Conditions](#) and the [Ethical guidelines](#) still apply. In no event shall the Royal Society of Chemistry be held responsible for any errors or omissions in this *Accepted Manuscript* or any consequences arising from the use of any information it contains.

Graphical Abstract

**Ultra Small Gold Nanoparticles Synthesis in Aqueous Solution and their application
in Fluorometric Collagen Estimation using Bi-ligand Functionalization**

Sankalp Vinod Agarwal#, Shyam Sunder Reddy#, Marshal Dhayal*



Ultra small hydrosol LBH-AuNPs were synthesized and their application in FRET based estimation of collagen using bi-ligand functionalised LBH-AuNP.

**Ultra Small Gold Nanoparticles Synthesis in Aqueous Solution and their application
in Fluorometric Collagen Estimation using Bi-ligand Functionalization**

Sankalp Vinod Agarwal#, Shyam Sunder Reddy#, Marshal Dhayal*
Clinical Research Facility, CSIR- Centre for Cellular and Molecular Biology, Uppal
Road, Hyderabad -500007, India.

* Corresponding Author (marshaldhayal@yahoo.com, Tel: +91-40-271-92500,
Fax: +91-40-271-27160591)

#Equal Contribution

Abstract:

An effective, rapid and facile hydrosol approach was developed to synthesize monodisperse ultra-small Gold nanoparticles (~2nm) by using Lithium borohydride (LiBH₄) as a reducing agent. These Lithium borohydride Gold nanoparticles (LBH-AuNPs) are highly stable at pH ranging from 2 to 10. We have subjected these LBH-AuNPs with bi-ligand co-functionalization with fluorescent FITC (Fluorescent isothiocyanate) and lysine molecules. It has been observed that these particles exhibit enhanced tolerant concentration of FITC and lysine bi-ligand functionalization. The fluorescence resonance energy transfers (FRET) of FITC and Lysine with AuNPs and ligand replacements of these fluorophores by collagen have been exploited for sensitive fluorometric detection of rat tail collagen. The linearity in reappearance of FITC and lysine fluorescence was observed at 2 to 10µg/ml of extracted rat collagen demonstrated the successful use of these bi-ligand surface functionalised gold nanoparticles as probe for the sensitive fluorometric estimation of rat tail collagen.

1. Introduction

Gold nanoparticles (AuNPs) have been used for various applications like biosensors, diagnosis, imaging system etc [1,2]. Particularly, the use of AuNPs for various applications in biomedical field are very common due to its potential to form the complexes with various biomolecules [3,4]. The Particles of small size are more preferred for these purposes, because of higher surface area /volume ratio [5], so that more concentration of plethora of biomolecules can be delivered, conjugated or sensed. Extensive work has been carried out to achieve stable and size controlled AuNPs by selecting appropriate reducing agents for the reduction of gold chloride salts [6]. Colloidal AuNPs of size 10-20nm have been commonly produced using the citrate method described by Frens in which size depend upon the citrate/HAuCl₄ ratio [7]. Furthermore, easy and rapid methods of AuNPs of small size (< 5nm) have been achieved by the reduction of AuCl₃ or HAuCl₄ with reducing agents like sodium borohydride (NaBH₄), hydrazine etc [8,9]. Recently, ultra-small nanoparticles (1-4nm) synthesis has been achieved in organic solvents [10]. In these synthesis, mono-dispersity and precise size were achieved with capping of alkane thiol-tethered polymeric ligands [11, 12]. However, these alkane thiols capping are toxic for most of the biological systems and also the use of organic solvents are not preferred due to environmental issues [13(a)]. Moreover, organic based AuNPs show poor water miscibility, which limits their usage in biological systems. Hence, the various approaches have been developed, but achieving hydrosol tuneable size AuNPs still faces a challenge.

The size dependent unique physical and chemical properties of nanomaterials have been exploited to generate and improve the colorimetric and fluorometric based

analytical methods [14]. In general, the dispersed AuNPs exhibit red or ruby colour solution, whereas aggregated and larger AuNPs display blue or purple colour solution [15]. On contrary to the dispersed AuNPs, the aggregated AuNPs have substantially lesser interparticle distance as compared to their average diameter [16,17]. As a result, these AuNPs display the colour change from red to blue colloidal solution. Thus, the change in colour of the solution is highly sensitive to the size, shape, refractive index of the medium, capping agents and the degree of aggregation of AuNPs [18]. In colorimetric based assays, the change in colour can be estimated by the shift in SPR (Surface Plasmon resonance). This principle has been utilized for ligand-metal ion complexes [15], antigen-antibody reactions [19] etc.

Furthermore, AuNPs showed greater molar extinction coefficient than organic dyes [20]. As a result, when fluorophores tagged molecules or fluorophores interact with AuNPs, their fluorescence will be quenched through the process of fluorescence resonance energy transfer (FRET). In FRET, the electron and/or energy transfer from the fluorophores to the AuNP leads to fluorescence quenching [21]. When the targeted analytes added to the fluorophores associated AuNPs, the fluorophores can be displaced or removed from the surface. As a result, the targeted analytes can be estimated with restored fluorescence of removed or displaced fluorophores from AuNPs. The intensity of fluorescence depends upon the concentration of the targeted analytes. This phenomenon has been used for various FRET based assays like competitive immunoassay of bio-molecules [19], detection of DNA hybridisation [22], ligand replacement induced fluorescence turn ON detection of pesticides [23] etc. However, the sensitivity of these applications depends on various factors like stability of nanoparticles against the tolerant concentration of targeted analyte, size, capping, monodispersity, solvents effect etc. For biological applications, there is need for the

hydrosol based synthesis of ultra small monodisperse AuNPs, which can display the stability against the above mentioned factor to achieve the sensitivity of the FRET based reaction.

Herein, we report a rapid, facile and hydrosol method of synthesis of monodisperse colloidal AuNPs with average diameter ~ 2 nm. To the best of our knowledge, this is the first study, where LiBH_4 is used as reducing agent for the aqueous synthesis of Gold nanoparticles. In AuNPs synthesis, stronger reducing agents provide smaller particle size [7, 8, 9]. According to literature, lithium based salts are stronger reducing agents due to highest negative reduction potential [24]. Therefore, LiBH_4 is considered as stronger reducing agent as compared to NaBH_4 [25]. Hence, we have used LiBH_4 for the synthesis of ultra small AuNPs than NaBH_4 . Further, LBH-AuNPs (Lithium Borohydride- Gold nanoparticles) were subjected to bi-ligand co-functionalization with fluorescent dye FITC and lysine molecules to obtain AuNP LBH-FITC-Lysine nanoparticles (AFL NPs) for the sensitive estimation of rat tail collagen through the FRET analysis (Fig.1). By the virtue of small size, these particles can tolerate the higher concentration of ligand molecules (here, FITC and lysine) as compared to the previous study [24]. Further, these particles can be used as a probe for the FRET based assay of bio-macromolecules like collagen. In this study, we have selected collagen estimation because only few colorimetric and fluorometric methods are available for collagen estimation like Sirius red test [27] and detection of collagen by intrinsic fluorescence [28]. Here, upon the addition of the collagen to the bi-ligand functionalised AFL NP, collagen induced the ligand replacement of FITC and lysine attached to AuNPs and restores their fluorescence (Fig 1). This turn ON fluorescence of FITC and lysine was found to be sensitive for the estimation of collagen with limit of detection (LOD) $2\mu\text{g/ml}$.

2. Experimental

2.1 Materials: Gold Chloride (AuCl_3), Lithium borohydride (LiBH_4), Collagen, L-lysine and Fluorescent isothiocyanate (FITC) were purchased from Aldrich-Sigma. The different pH solutions were prepared by mixing different volumes of NaOH and HCl. All the experiments were performed in Milli-Q water (Merck- millipore, USA). Average LBH AuNPs diameter, frequency distribution of LBH-AuNPs size and standard deviation were calculated for each sample of nanoparticles by averaging atleast 100 nanoparticles from TEM image using Image J software (developed by National Institute Health) [29,37].

2.2 Instruments: The double beam Perkin Elmer Lambda 35 Spectrophotometer was used for UV-Visible absorption spectra. Fluorescence emission spectra were obtained with Hitachi 4500 Japan spectrophotometer having slit width of 5nm. Excitation and emission wavelengths of FITC and L-Lysine are 488nm, 355nm and 520nm, ~435nm respectively. The TEM micrographs of AuNPs and modified AuNPs with Lysine, FITC and collagen were obtained by 200KV Transmission Electron Microscope, from JEOL, Japan. . All measurements were conducted in triplicate. The median value and S.D was considered for plotting the graphs.

2.3 Preparation of LiBH_4 synthesised Gold nanoparticles (LBH-AuNP) and pH stability

A series of LiBH_4 solutions were prepared with final concentrations (a) 0.33mM, (b) 0.66mM, (c) 1.32mM, (d) 2.64mM, (e) 5.28 and (f) 7.92mM in 248ml Milli Q water. To this, 2ml of 1% (w/v) AuCl_3 solution was added with vigorous stirring for few minutes and colloidal Gold nanoparticles were formed. The gradual changes in blue to

red colour colloidal solutions were observed with LiBH_4 concentration ranging from 0.33mM to 7.92mM. Here, we have considered the optimum AuNPs synthesized with 2.64mM of LiBH_4 and used for all the experiments. The concentration of optimum AuNPs was found to be 1.3 μM [30] SI: 1 (Detailed calculation is given in supplementary information). The particles synthesized in Milli Q water with 2.64mM of LiBH_4 have pH \sim 7.4. Further, stability of the optimised LBH-AuNP was studied by gradually changing the pH using 1N HCl and 1N NaOH ranging from pH 3 to 10.6

2.4 Preparation of bi-ligand functionalized AuNP LBH -FITC-Lysine (AFL NPs) and mono functionalized AuNP LBH – FITC (AF), AuNP LBH -lysine (AL) nanoparticles

The bi-ligand functionalised AFL NPs were synthesised in two steps. (a) To the 5ml of 1.3 μM of AuNPs solution 50 μl of 500 μM FITC solution (Dissolved in 95% ethanol) was added with final concentration of 5 μM FITC in AuNPs and incubated for 30 mins. Next, 100 μl of 100mM of lysine (solution 'b') added with final concentration of 2mM lysine in solution (a) and incubated for 30 mins. In both reactions (a) and (b) saturated concentration of FITC (500 μM) and lysine (100mM) were used respectively. Similarly, for AF and AL solutions preparation, 5ml of 1.3 μM AuNPs solution contain final concentration of 5 μM FITC and 2mM of lysine respectively. All the reactions were incubated for 30 min at room temperature.

2.5 Fluorometric assay of collagen using AFL, AF and AL nanoparticles

A series of collagen concentration was prepared in 2ml of AFL, AL and AF nanoparticles with final concentration 2 to 10 $\mu\text{g}/\text{ml}$ from 100 $\mu\text{g}/\text{ml}$ of stock collagen solution. For the real time collagen estimation, rat tail collagen was extracted followed by Navneeta Rajan et. al, [31] and concentration was adjusted to 1 mg/ml by Sirius red

test [32] The respective AFL, AL and AF containing collagen solutions were incubated overnight at 4°C. These reactions were analysed and characterized by fluorescence spectrometry.

3 Results and discussion

3.1 Synthesis of ultra small LBH-AuNPs by LiBH₄ reduction

UV-Vis spectra of LBH-AuNPs synthesized with different concentrations of LiBH₄ ranging from 0.33mM to 7.92mM showed in Fig 2A. The increase of LiBH₄ concentration caused shift in SPR peak from 573nm to 512nm (a-f). The corresponding colour changes from blue to red colloidal solutions were observed as shown in Fig 2B.

According to Martin et. al, NaBH₄ naked synthesis of stabilizer free colloidal AuNPs may have anion capping of boron based ions [33]. However it is not yet confirmed. In this synthesis, where LiBH₄ was used, similar negative charged capping of the AuNPs is expected, which render the colloidal nature of these particles. From the SPR spectra, the gradual blue shifts with increase in LiBH₄ indicate the corresponding reduction in AuNPs size. As per the literature, with increase in particle size, the SPR shows shift toward longer wavelength [33]. To estimate the particle size from SPR of these AuNPs, we have used an established experimental model based on multipole scattering to estimate the particle size from spectroscopic observation of AuNPs [30]. However, in this study the model explained for the estimation of the larger and polydisperse LBH –AuNP was not found in correlation with observed size of AuNP in TEM image with large % error, but showed consistency with small sized AuNPs. From the UV-Visible spectra the LBH-AuNP synthesised in conditions (d-f) have greater blue shift as compared to conditions (a-c). Thus, smaller and narrow distribution of the particles can be expected in former samples than latter one. Smaller nanoparticles diameter was estimated by measuring absorbance at $\lambda_{spr}/\lambda_{450}$ as described by Haiss et al [30]. The observed λ_{spr} of LBH-AuNPs synthesised at 2.64mM (d), 5.28mM (e)

and 7.92mM (f) of LiBH_4 concentrations were at 512nm, 510nm and 520nm, respectively. The corresponding estimated sizes of the LBH-AuNPs were $\sim 4\text{nm}$, $\sim 4\text{nm}$ and $\sim 5\text{nm}$. Further, TEM analysis was carried out to accurately estimate the size of AuNPs synthesized at various LiBH_4 concentrations and results are showed in Figure 3 (a-f).

From the TEM analysis, the particle synthesised at lower LiBH_4 concentrations (a-c) showed larger and/or aggregated AuNPs ($\sim 5\text{nm}$ to $\sim 35\text{nm}$). This can be evident from the shifts and broadened SPR peaks of the corresponding AuNPs. As a result, the abovementioned model cannot be used for these polydisperse AuNP. On the contrary, the particles synthesised with increase LiBH_4 concentration (d-f) exhibit smaller average particles size $2.2 \pm 0.4\text{nm}$, $3.4 \pm 0.3\text{nm}$ and $3.7 \pm 1.3\text{nm}$ respectively, accumulated by frequency distribution graph using image J software as observed from insets showed in Fig 3 (d-f). Thus, the particles synthesized at higher LiBH_4 concentrations were showed very good consistence in their diameter obtained from TEM and spectroscopic observations. Here, we have found the particles synthesised with 2.64mM LiBH_4 showed remarkable stability at room temperature for more than six months, whereas other precipitated. In general, the stable colloidal AuNPs have been achieved at optimum ratio of metal precursor to reducing agents [7]. Particles synthesised from this optimised condition was used to perform the below mentioned experiments.

3.2 Stability of LBH-AuNPs with different pH

Initial pH of the colloidal solution of these particles synthesized with 2.64mM of LiBH_4 was ~ 7.4 . Stability of these LBH-AuNPs at different ionic strengths was estimated by changing pH from 3 to 10.6. The pH was adjusted by using 1N HCl and 1N NaOH. From Fig 4A, the LBH-AuNPs showed overall slight red shift in SPR peak of $\sim 3\text{nm}$ at pH 3, 5, 7, 9 and 10.6 (a-e). Furthermore, these particles at corresponding pH maintain the colloidal nature as

shown in Fig 4B (a-e). These observations confirm higher stability of these particles in both acidic and basic conditions.

3.3 Bi-ligand functionalization of LBH- AuNPs with Lysine and FITC

According to shukla et. al., the attachment of Lysine and FITC to the sodium borohydride synthesised AuNPs had been explained [24]. In this surface functionalization, -NCS group of FITC interacts with AuNP [2], whereas at physiological pH α -NH₂ of lysine interacts with AuNP [13a] Here, similar functionalization was performed with LBH-AuNPs. However, in previous study, the conjugations of lysine and FITC to AuNPs were explained by FRET of FITC. In this study, we are first time introducing FRET of Lysine (Ex/EM: 355/~410-435nm) and FITC (Ex/Em:488/520nm) to explain the bi-ligand functionalization of LBH-AuNPs with FITC and Lysine to get LBH-AuNP-FITC-Lysine nanoparticles (AFL nanoparticles). In this study, we have selected lysine and FITC molecules due to few reasons; First, Lysine and FITC are fluorescent molecules and functionalization of these molecules can be monitored by FRET and ligand replacement reactions. Second, fluorescence of these molecules can be used for the fluorometric estimation of bio-macromolecules. As per reported literature, lysine at higher concentration (> 10mM) showed broader peak of fluorescence at ~ 435nm [34], which is overlapping with Raman water peak at 405nm. However, at lower lysine concentration (\leq 2mM), a shoulder broad lysine fluorescence peak at ~435nm to water raman peak can be distinctly observed as shown in Fig 5(II).

In the FRET study of AFL nanoparticles, individually fluorescence of FITC (5 μ M) and Lysine (2mM) molecules (Fig 5I(a) and II(a)) showed overall fluorescence quenching with AuNPs (1.3 μ M) to achieve (AF) and (AL) nanoparticles as showed in Fig 5 (IIa and IIb) respectively. Here, FRET of Lysine and FITC with AuNP were separately observed to have better understanding about bi-ligand functionalization of LBH-AuNPs. In AFL nanoparticles

preparation, lysine was added to AF nanoparticles. This results in the functionalization of AF particle with Lysine to get bi-ligand AFL nanoparticles. Upon the addition of lysine to AF nanoparticles, the restored fluorescence of replaced FITC and unbound residual lysine fluorescence have been observed as shown in Fig .5I(b) and II (b) , which corresponds to the to 2.3% (0.115 μ M) and 4.3% (85 μ M) of free and/or replaced FITC and lysine concentrations respectively. Hence, more than 95% of both molecules co-functionalization has been achieved with LBH-AuNPs. The concentrations of residual FITC and Lysine were calculated by the standard graphs given in SI: 2.

Moreover, the above foresaid functionalizations were confirmed by UV-visible spectroscopy. From the Fig 6I :(a-d), the red shift of surface plasmon resonance (SPR) peak from 512nm to 545nm was observed with corresponding functionalization namely, (a) AuNP alone, (b) AuNP-FITC (AF), AuNP-Lysine (AL) and AuNP-FITC-Lysine (AFL). The inset is showing the corresponding colour change from red to blue colloidal solutions (a-d). This shift toward longer wavelength can be attributed to increase in size and/or aggregation of the particles. This result was confirmed by TEM analysis. The TEM images of the corresponding samples are showed in Fig. 6II (a-d).

From the comparison of TEM images Fig 6II(a-d), as compared to LBH particles alone, AuNP-FITC (AF) showed meagre change in particles size, whereas AuNP-lysine (AL) functionalised particles showed open chain string morphology. This morphology was observed due to formation in interparticle hydrogen bonding between lysine functionalised AuNPs [24]. In case of co-functionalization of AuNP with lysine and FITC showed still greater degree of aggregation and/or increase in particle size. This gradual change in the size and aggregation of the particles would explain the gradual shift of SPR and broadening of peaks of the corresponding functionalised AuNPs Fig 6I(a-d). Therefore, UV-Visible and

TEM analysis explain the singly and bi-ligand functionalization of LBH-AuNPs with lysine and FITC.

3.4 Fluorometric estimation of Rat tail collagen using bi-ligand functionalised AFL nanoparticles

According to recent literature, AuNPs crosslink and immobilize the collagen by nucleation process, which has been used for building bio-active surfaces for tissue engineering [35]. In this study, the nucleation properties of AuNPs with collagen have been used for the rapid and sensitive fluorometric based estimation of collagen by using AFL nanoparticles. Herein, we have used the Co-functionalized AFL particle for the quantification of collagen by ligand replacement reaction. The commercial Type-I rat tail standard collagen (P) was used with varying concentrations ranging from 2 to 10 μ g/ml. The FITC and Lysine fluorescence recovery has been observed to be highly linear with corresponding collagen (P) concentrations of 2 to 10 μ g/ml as shown in Fig 7(A&B).

The complete spectra are given in supplementary information SI: 3(a). However, the precipitation of the reaction was observed at higher concentration of collagen (20 μ g/ml). This can be evident from the representative TEM images of AFL NPs at collagen concentrations (2 and 20 μ g/ml) and colloidal image of these concentrations as showed in supporting information SI: 3(b), where 2 μ g/ml collagen remained in colloidal state, whereas 20 μ g/ml collagen showed precipitation. Furthermore, similar reaction was performed with extracted rat tail collagen [31] and adjusted to 1mg/ml by the Sirius red method [27]. (Standard graph of collagen by Sirius red method is given in SI: 3(c). The linearity in reappearance of FITC and lysine fluorescence from 2 to 10 μ g/ml has been observed with extracted rat tail collagen (RT) as shown in Fig.7A and B, respectively. The recovery response curve of FITC and lysine with different concentrations of rat tail collagen and pure standard collagen showed

similar quantification and detection sensitivity (10.3 ± 0.4 and 0.34 ± 0.04 fluorescence units/ $\mu\text{g/ml}$) for FITC and lysine, respectively). The % recovery of different concentrations of rat tail collagen with concomitant reappearance of lysine and FITC fluorescence is showed in Table I and II respectively, as shown in supplementary information SI: 3(d). This linearity in reappearance of FITC and Lysine fluorescence with increase concentration of collagen could be attributed to controlled aggregation of AFL particles with collagen. This aggregation of AFL AuNPs with collagen matrix may occurred as a result of interaction of side chain of lysine, hydroxy-lysine and hydroxyl-proline residue of collagen fibrils [36] with AFL particles, which could possibly lead to the controlled replacement of AuNP surface attached fluorescent lysine and FITC molecules. As a result, bi-ligand functionalised AuNPs showed linear reappearance of fluorescence of FITC and lysine with increase in concentration of collagen. To further demonstrate the usefulness of bi-ligand functionalised AuNPs, similar experiments were performed with mono-functionalised AuNP-lysine and AuNP-FITC respectively, as shown in SI: 3 (e). However, similar linear responses in reappearance of lysine and FITC fluorescence with standard collagen (P) have not been observed with mono-functionalised AuNP-lysine and AuNP-FITC. Therefore, bi-ligand functionalised LBH-AuNPs were found to be more sensitive and efficient for the fluorometric estimation of collagen. Moreover, fluorescence reappearance of both Lysine and FITC from AFL AuNPs provide additional confirmation for estimation of collagen. Thus, these bi-ligand surface modified LBH AuNPs (AFL particle) have been successfully used for the sensitive fluorometric quantification of rat tail collagen.

Conclusions

In summary, a unique, rapid and facile hydrosol synthesis of highly dispersed AuNPs with size of $\sim 2\text{nm}$ has been achieved by using LiBH_4 as reducing agent. Due to small particle size and stability at different physio-chemical conditions renders these particles suitable for bi-

ligand co-functionalization with higher concentration of fluorescent Lysine and FITC molecules. The collagen induced controlled aggregation of AFL particles were successfully used for fluorometric quantification of rat tail collagen. Thus, this uniquely synthesized AuNPs bestow most of the desired characteristics, and can be used for the wide range of applications.

Acknowledgements

This work was financial support from Department of Biotechnology, Ministry of Science and Technology, Govt. of India (BT/PR13243/GBD/27/227/2009). We are thankful to Dr Gopal Pande, CCMB for useful discussion and lab space.

Supplementary Information:

Electronic Supplementary Information (ESI) on calculation of the concentration of optimised LBH-AuNPs, fluorescence standard graphs of Lysine and FITC, TEM and optical image of collagen-AFL nanoparticles and standard graph of extracted rat tail collagen are available.

References

1. Min Sik Eom, Woojeong Jang, Yoon Seo Lee, Gildon Choi, Yong-Uk Kwon and Min Su Han, *Chem. Commun*, 2012, 48, 5566.
2. Yi-Ming Chen, Tian-Lu Cheng and Wei-Lung Tseng, *Analyst*, 2009, 134, 2106–2112.
3. Feng Wang, Yu-Cai Wang, Shuang Dou, Meng-Hua Xiong, Tian-Meng Sun, and Jun Wang, *ACS nano*, 2011, 5, 3679–3692.
4. Xiangyang Shi, Su He Wang, Mary E. Van Antwerp, Xisui Chenb and James R. Baker, *Analyst*, 2009, 134, 1373–1379.
5. Dingbin Liu, Zhuo Wang and Xingyu Jiang, *Nanoscale*, 2011, 3, 1421-1433.
6. Handley.D, *Principles, Methods, and application* 1989, 11, 13-32.

7. Frens, G. *Nature Phys. Sci.* 1973, 241, 20-22.
8. Akshaya K. Samal, Theruvakkattil S. Sreepasad, Thalappil Pradeep, *J Nanopart Res*, 2010. 12, 1777–1786.
9. Angshuman Pal, Sunil Shah, Surekha Devi, *Colloids and Surfaces A: Physicochem. Eng. Aspects*, 2007, 302, 51–57.
10. Yong Yu, Zhentao Luo, Yue Yu, Jim Yang Lee, and Jianping Xie, *ACS nano*, 2102,6, 7920–7927.
11. Huifeng Qian, Yan Zhu, and Rongchao Jin, *PNAS*, 2011, 1-5.
12. I. Hussain, S. Graham, Z. Wang, B. Tan, D. C. Sherrington, S. P. Rannard, A. I. Cooper, M. Brust, *J. Am. Chem. Soc.* 2005, 127, 16398-16399.
13. (a) R. Lévy, N. T. K. Thanh, R. C. Doty, I. Hussain, R. J. Nichols, D. J. Schiffrin, M. Brust, D. G. Fernig, *J. Am. Chem. Soc.* 2004, 126, 10076, (b) P. Selvakannan, S. Mandal, S. Phadtare, R. Pasricha, M. Sastry, *Langmuir* 2003, 19, 3545
14. Dingbin Liu, Zhuo Wang and Xingyu Jiang, *Nanoscale*, 2011, 3, 1421.
15. Min Sik Eom, Woojeong Jang, Yoon Seo Lee, Gildon Choi, Yong-Uk Kwonz and Min Su Han, *Chem. Commun.*, 2012, 48, 5566–5568
16. R. Klajn, J. F. Stoddart and B. A. Grzybowski, *Chem. Soc. Rev.* 2010, 39, 2203–2237.
17. S. K. Ghosh and T. Pal, *Chem. Rev.*, 2007, 107, 4797–4862.
18. M. C. Daniel and D. Astruc, *Chem. Rev.*, 2004, 104, 293–346.
19. Peihui Yang et.al, *American Journal of Analytical Chemistry*, 2011, 2, 484-490
20. G. A. Rance, D. H. Marsh and A. N. Khlobystov, *Chem. Phys. Lett.*, 2008, 460, 230–236.
21. K. G. Thomas and P. V. Kamat, *Acc. Chem. Res.*, 2003, 36, 888–898.

22. Paresh Chandra Ray, Angela Fortner, and Gopala Krishna Darbha, *J. Phys. Chem. B*, 2006, *110*, 20745-20748.
23. Kui Zhang et. al, *Anal. Chem.* 2010, *82*, 9579–9586.
24. Ravi Shukla, Vipul Bansal, Minakshi Chaudhary, Atanu Basu, Ramesh R. Bhonde, and Murali Sastry, *Langmuir* 2005, *21*, 10644-10654.
25. John Kotz, Paul Treichel, Gabriela Weaver, *Chemistry and Chemical Reactivity, Enhanced Review Edition*, 2006, 1328.
26. Robert F. Nystrom, Saul W. Chaikin, Weldon G. Brown, *J. Am. Chem. Soc.*, **1949**, *71* (9), 3245–3246.
27. Marcello marota, Guglielmo martino, *Analytical biochemistry*, 1985, *150*, 86-90.
28. Irene Georgakoudi, Brian C. Jacobson, Markus G. Müller, Ellen E. Sheets, Kamran Badizadegan, David L. Carr-Locke, Christopher P. Crum, Charles W. Boone, Ramachandra R. Dasari, Jacques Van Dam, and Michael S. Feld, *Cancer research*, 2002, *62*, 682–687.
29. Xiong Liu, Mark Atwater, Jinhai Wang, Qun Huo, *Colloids and Surfaces B: Biointerfaces* 2007, *58*, 3–7.
30. Wolfgang Haiss, Nguyen T. K. Thanh, Jenny Aveyard, and David G. Fernig, *Anal. Chem.* 2007, *79*, 4215-4221.
31. Navneeta Rajan, Jason Habermehl, Marie-France Coté, Charles J Doillon & Diego Mantovani, *Nature Protocols*, 2007, *1*, 2753 – 2758.
32. Marcello marota, Guglielmo martino, *Analytical biochemistry*, 1985, *150*, 86-90.
33. Matthew N. Martin, James I. Basham, Paul Chando, and Sang-Kee Eah, *Langmuir* 2010, *26*(10), 7410–7417
34. L. Homchaudhuri and R. Swaminathan, *Chemistry Letters*, 2001, 844-845.

35. Santosh Aryal, Remant Bahadur K. C, Shanta Raj Bhattarai, P. Prabu and Hak Yong Kim, *J. Mater. Chem.*, 2006, 16, 4642–4648.
36. Daniel Gottlieb, Stephen A. Morin, Song Jin and Ronald T. Raines, *J. Mater. Chem.*, 2008, 18, 3865–3870.
37. Matthew S. Lamm, Nikhil Sharma, Karthikan Rajagopal, Frederick L. Beyer, Joel P. Schneider and Darrin J. Pochan, *Adv. Mater.* **2008**, 20, 447–451.

Figure Captions:

Figure 1: The schematic representation of LiBH_4 synthesized AuNPs, bi-ligand surface modified AuNPs with FITC (Ex/Em: 488/520) and Lysine (Ex/Em: 355/~435) to form AFL nanoparticles and fluorometric estimation of rat tail collagen by reappearance of FITC and lysine fluorescence from AFL nanoparticles. The release and restore fluorescence of FITC and lysine was attributed to the controlled nucleation of AFL nanoparticles with collagen.

Figure 2: (A) UV-Vis spectra (B) Colloidal-LBH-AuNPs synthesised at LiBH_4 concentrations, (a) 0.33mM, (b) 0.66mM, (c) 1.32mM, (d) 2.64mM, (e) 5.28mM and (f) 7.92mM.

Figure 3: TEM images of LBH-AuNPs synthesised at (a) 0.33mM, (b) 0.66mM, (c) 1.32mM, (d) 2.64mM, (e) 5.28mM and (f) 7.92mM of LiBH_4 concentrations. Inset showing frequency distribution graphs.

Figure 4: UV-visible spectra of LBH-AuNPs at different pH solution (a) pH 3, (b) pH 5, (c) pH 7, (d) pH 9 and (e) pH 10.6. (B) Optical images of corresponding colloidal LBH-AuNPs from (a) - (e).

Figure 5: Functionalization of AuNPs with L-lysine, FITC, FITC and L-lysine. (I) FITC fluorescence (Ex/Em-488/520nm) of (a) FITC, (b) AuNP-FITC (AF) and (c) AuNP-FITC-Lysine (AFL). Inset showing magnifying spectra of b & c. (II) Lysine fluorescence (Ex/Em-

355/~435nm) of (a) Lysine, (b) LBH-AuNP-Lysine (AL) and (c) LBH AuNP-FITC-Lysine (AFL).

Figure 6: (I) UV-Visible spectra of functionalized nanoparticles (a) AuNP, (b) AuNP-FITC (AF), (c) AuNP-Lysine (AL), (d) AuNP-FITC-Lysine (AFL) with inset showing corresponding optical picture. (II) TEM images of corresponding functionalised particles from (a) to (d).

Figure 7: Reappearance of fluorescence of FITC and Lysine from AuNP-FITC-Lysine (AFL) nanoparticles with different concentration of collagen varying from 2 μ g/ml to 10 μ g/ml. (A) and (B) represent the data associated with FITC and lysine fluorescence reappearance, respectively. $I_F(P)_C$ associated with fluorescence peak intensity in presence of collagen and $I_F(P)_0$ associated with fluorescence peak intensity without collagen. Collagen (P) represent data associated with pure collage obtained from Aldrich-Sigma and Collagen (RT) represent data associated with rat rail extracted collagen.

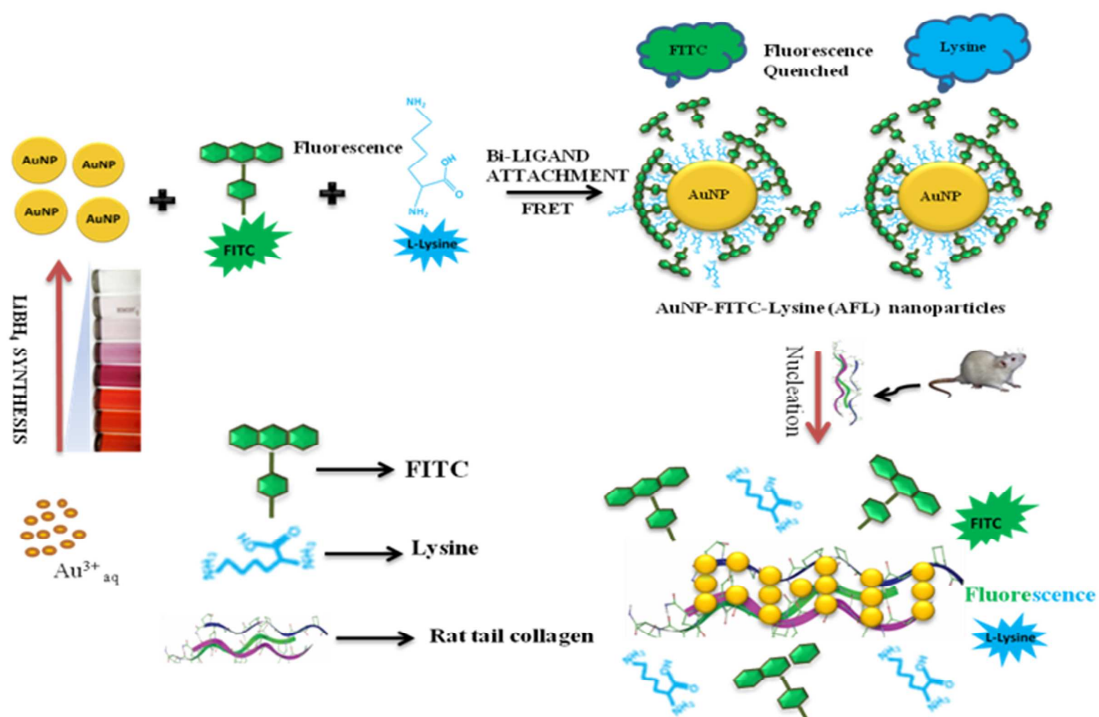


Figure 1

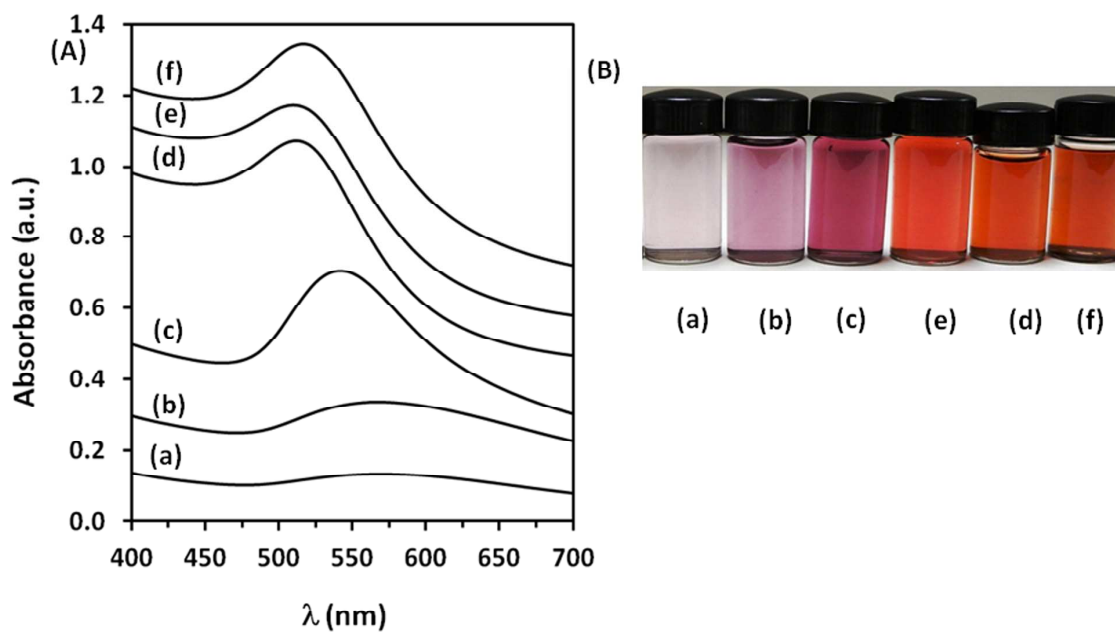


Figure 2

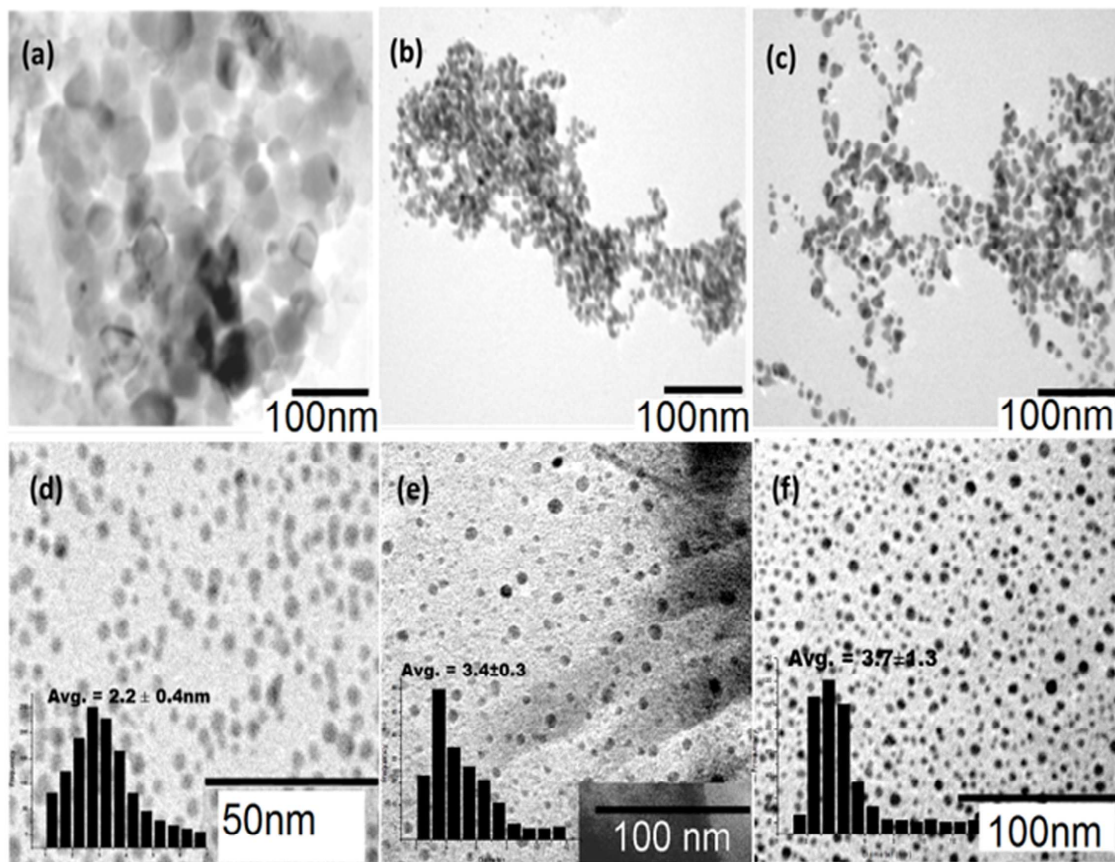


Figure 3

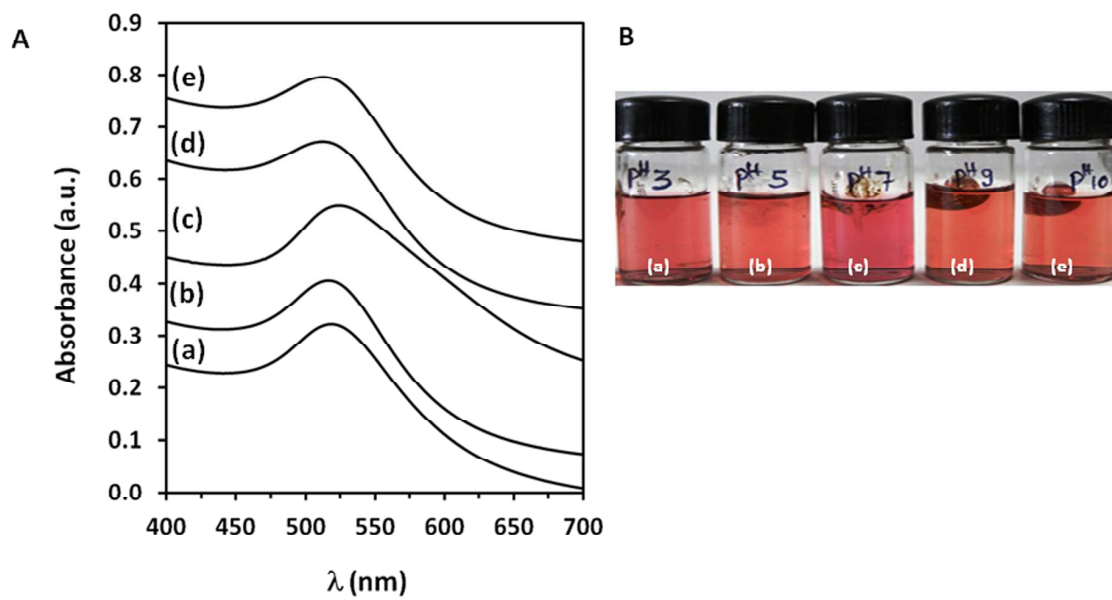


Figure 4

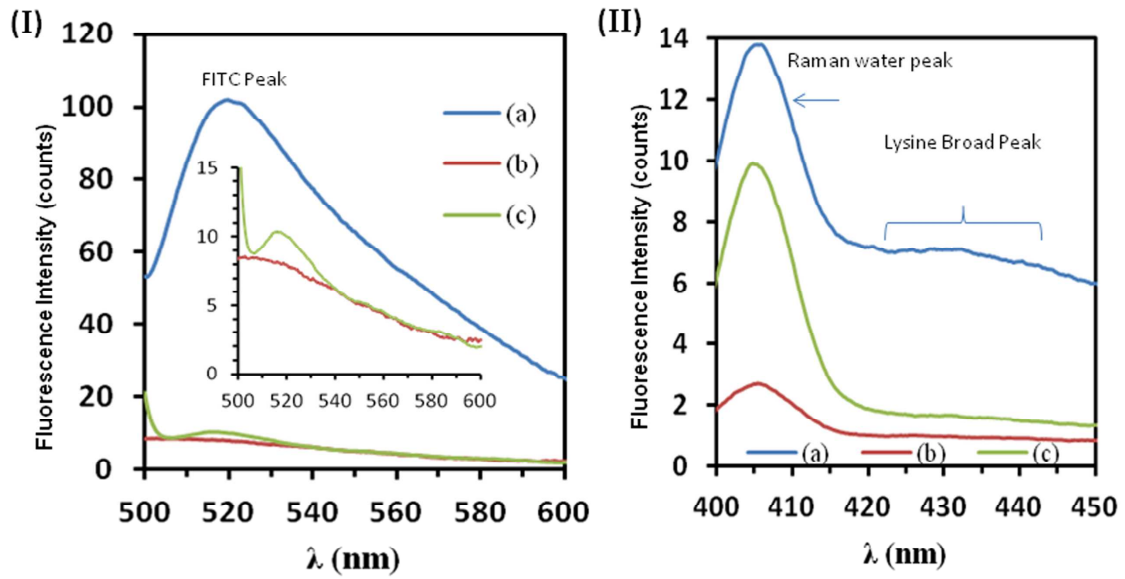
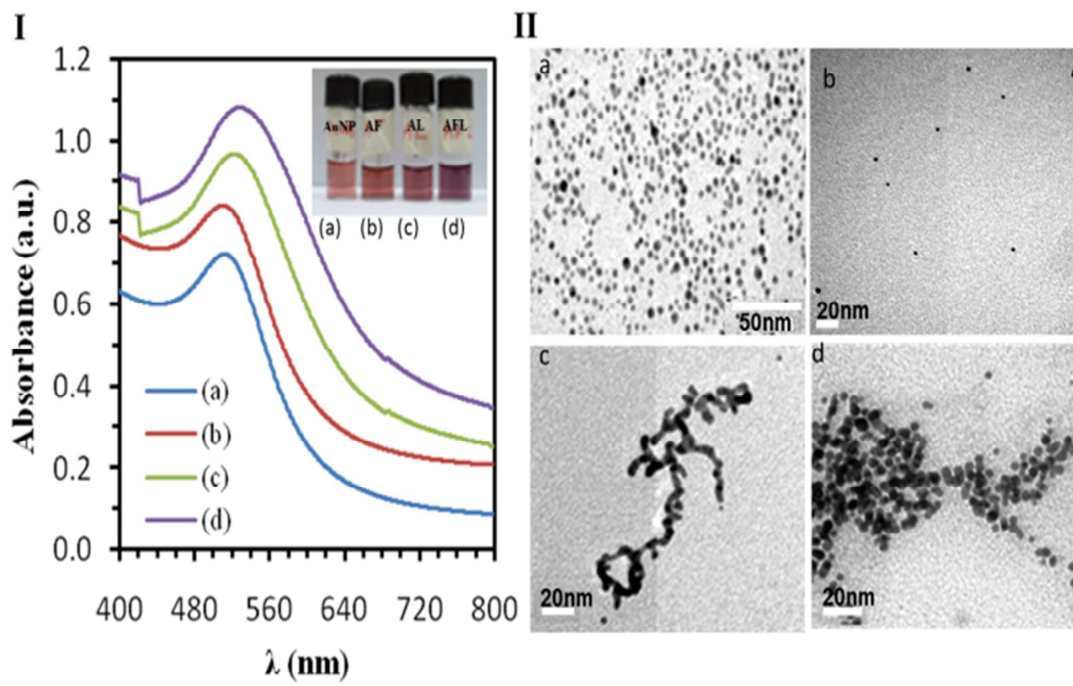


Figure 5



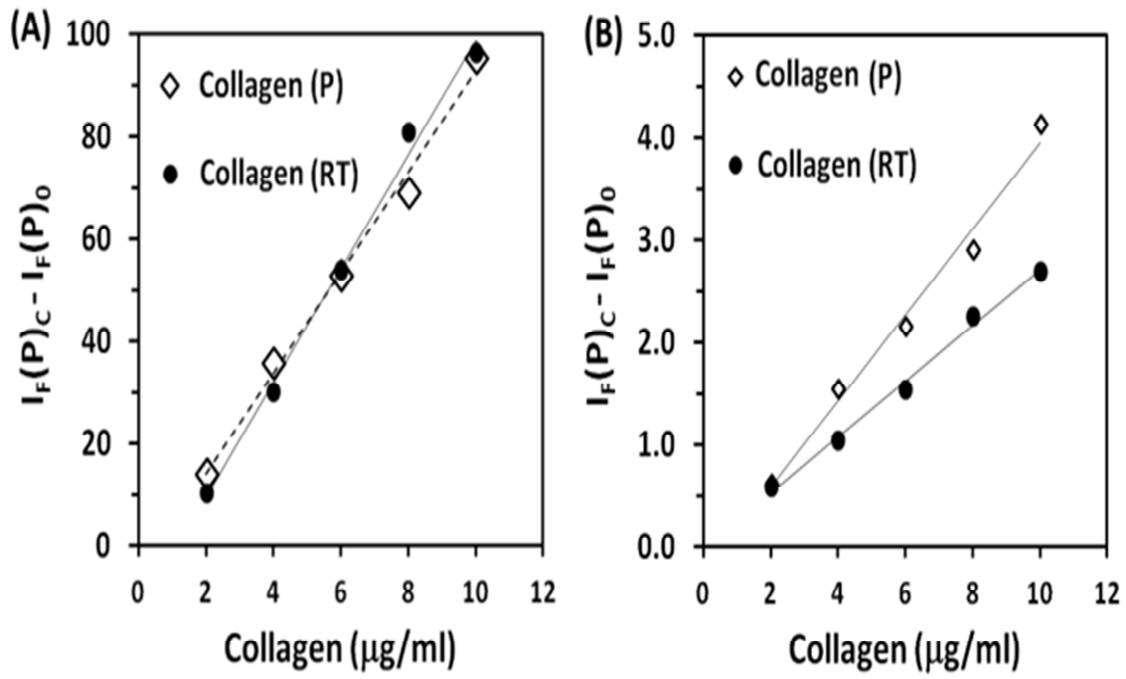


Figure 7